BULLETIN OF THE POLISH ACADEMY OF SCIENCES
TECHNICAL SCIENCES, Vol. 63, No. 4, 2015
DOI: 10.1515/bpasts-2015-0108

Adaptive, compensating control of wheel slip in railway vehicles

J. KABZIŃSKI*

Institute of Automatic Control, Lodz University of Technology, 18/22 Stefanowskiego St., 90-924 Lodz, Poland

Abstract. The problem of slip stabilization and tracking in railway vehicle applications is considered. A nonlinear adaptive control compensating for unknown disturbance in motion dynamics such as: friction, contact force variations and air resistance is proposed. The control is based on approximate models with adaptive parameters. The stability of several control algorithms is proven and performance of the derived controllers is investigated. The proposed controllers are evaluated in numerical simulations and by DSP application to slip control in a friction gear driven by a permanent magnet synchronous motor.

Key words: adaptive control, slip compensation, railway traction drives.

1. Introduction

The tangential force exerted during wheel-rail contact is commonly referred to as "adhesion force", while the ratio between the adhesion force and the normal force is known as the adhesion coefficient. Operation with maximal adhesion force is one of the most important problems in the control of propulsion drives for railway vehicles. Due to special contact conditions between the wheel and the railway under huge normal forces, the adhesion coefficient is a function of slip and velocity, as presented in Fig. 1. Acting with too small values of slip results in insufficient adhesive force. Operation on the decreasing slope of the surface presented in Fig. 1 produces lower contact force with increasing slip and may cause system instability, if linear (PI or PID) motion controllers are applied. During an attempt to accelerate a vehicle, this produces heat or sparkling, destroys the wheel and rail surfaces and may make acceleration impossible. In braking mode, the wheel may be blocked, which makes it slip on the rail, changing the circular shape of the wheel. Operation with excessive slip decreases the efficiency of energy conversion and leads to the costly repairs of trains and rails.

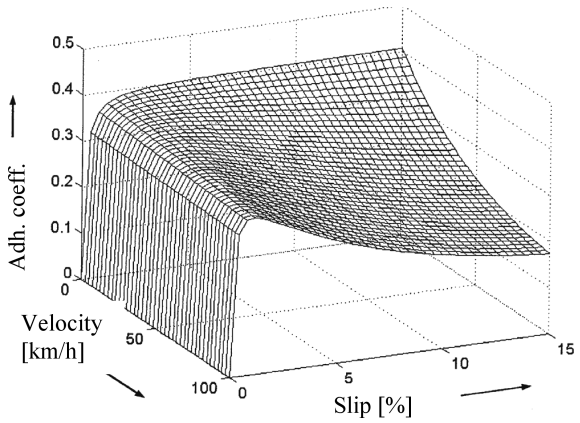

Fig. 1. Adhesion force coefficient as a function of wheel slip and velocity according to the model given in Ref. 1

The aim of the proposed control algorithm is to stabilize the slip value that provides adhesive force maximization. Slip depends on actual train velocity and railway conditions [1, 2], and identification of the exact value is a difficult and complex problem. Nevertheless, it is relatively easy to estimate the slip value that leads to the adhesive force that is sufficiently close to the maximal value under a wide range of external conditions. Stabilization of such a slip value (if robust for any value on the decreasing or the increasing slope of the slip-adhesion force curve) provides acceptable drive performance. For this reason, the slip stabilization problem is an important issue. Regardless, generalization in the context of the slip tracking problem is considered in the present paper.

Slip stabilization must be robust against uncertainties and variations in any of the drive model parameters. For example, the wheel radius may change by several percent during the wheel's lifetime. The adhesion coefficient depends on the railway conditions (wet or dry, contaminated with lubricants); train mass changes according to load or number of passengers; the resistance force caused by the motion of the train depends on the wind force and direction, as well as the slope and curvature of the rail; even the normal force oscillates due to suspension dynamics and changes because of the rail slope variations, or the rail or wheel irregularities [2]. All of these factors legitimize application of adaptive control in order to stabilize the slip.

It has been evident for many years that a special control strategy must be used to cope with slip in railway traction. With the increasing speed of vehicles, this problem becomes ever more important. The first concept of anti-slip, re-adhesion control was to detect an excessive slip and to apply torque reduction according to a predefined pattern [3]. Slip detection may be based on the analysis of several signals: velocity, acceleration, vibrations or noise spectrum [4], or motor current [5, 6]. PI controllers were widely applied, usually with linear observers of the adhesion coefficient, adhesion coefficient derivative, or adhesion force [7–9]. It was noticed, however,

*e-mail: jacek.kabzinski@p.lodz.pl

that linear controllers do not guarantee stability if for any reason the system operates with a negative slope of the slip curve. Therefore, modern nonlinear control techniques have been proposed to achieve contact force maximization. It has been observed that a fuzzy controller can be used instead of torque reduction [3].

The problem of the desired train position and velocity tracking was investigated in [10–12]. Such an approach may only be applied under the assumption that reference trajectories implicate that the desired adhesive force is always available. A sliding mode approach [13] was intensively investigated, although it suffers from typical drawbacks such as high switching torque frequency. Recently, the immersion and invariance technique was used [14] with promising results. However, it requires a special form of adhesive coefficient curve, some parameters must be known and the train velocity is assumed to be varying slowly. As is evident from this discussion, each approach has some drawbacks and as such, the investigation of other methods is justified.

In this paper a new control strategy is proposed, based on adaptive compensation of the unknown components in slip dynamics equations. The controller operates using linearly parameterized models of all disturbances present in system dynamics: rotational friction, contact force and linear motion resistance. It is not assumed that the models are accurate – it is sufficient if the modelling error is bounded. Additionally, no special structure of real contact force or friction acting on the system is required. Several control algorithms for slip tracking, as well as for the slip velocity tracking problem, are investigated and compared.

The paper is organized as follows: in Sec. 2, the problem is formulated (2.1) and several control algorithms of slip stabilization are derived and their stability in the UUB sense is proven (2.2); finally, a control approach with slip velocity tracking is discussed (2.3). In Sec. 3, some simulations evaluating the performance of the proposed control are presented and the control implementation within the laboratory stand with a friction gear driven by a permanent magnet synchronous motor (PMSM) is described.

2. Control algorithms

2.1. Problem statement. The longitudinal dynamics of the train body may be represented as a chain of k vehicles joined by $N-1$ nonlinear, elastic couplings with p motors. This representation leads to the so-called "multi mass model" [12] that accounts for in-train forces. As in-train forces are extremely difficult to measure and model, the simplified model that neglects the coupling elasticity and the motor-wheel transmission dynamics is commonly accepted [2, 12–14]. The single-mass, single motor model is given by

$$J\frac{d}{dt}\omega = T_N - RF_a - T_f, \tag{1}$$

$$M\frac{d}{dt}v = F_a - F_f, \tag{2}$$

$$F_a = \mu_a N, \tag{3}$$

where M is the vehicle mass corresponding to the driving axle, v – linear velocity, J – the wheel inertia, ω – rotational speed, R – the wheel radius, T_N is the motor torque (thrust or braking), T_f is the friction torque affecting the motor and F_f is the resistance force caused by the motion of the vehicle and the air drag. The contact (adhesion) force F_a is proportional to the normal force N. The adhesion coefficient μ_a is a function of the wheel slip, which is defined as

$$s = \frac{\omega R - v}{v} = \frac{\omega R}{v} - 1, \tag{4}$$

or, according to some investigations [1, 15], a function of slip and linear velocity, as it is presented in Fig. 1.

The coefficient μ_a depends on many factors such as the presence of water and contaminations on the railway, railway or wheel shape and many others. The typical curve of $\mu_a(s)$ can be found in [15] and the bibliography therein. It must be stressed that the information about this curve is very uncertain, although the primary features are: $\mu_a(s)$ is anti-symmetric, it possesses extrema $\pm\mu_{\max}$ for $s = \pm s_{\max}$, converges to zero for slip tending to zero and approaches constant asymptote for a big negative or positive slip. For wet railways, $\mu_{\max}$ decreases significantly, while $s_{\max}$ decreases slightly. Information about the actual adhesive force can be obtained from various types of observers [3, 4, 6, 12] and in this way, approximate information about $s_{\max}$ is provided.

The aim of control is to maximize the adhesion force stabilizing the actual slip around $s_{\max}$ by following the reference value s_d. In the present contribution, the way for calculating s_d is not discussed in detail; instead, the presentation concentrates on the tracking problem. It is assumed that the desired slip trajectory s_d is smooth and that the derivative $\dot{s}_d$ is available.

Generally, motors' electrical time constants are much smaller than the mechanical time constants of a railway vehicle. Therefore, in some applications, dynamics of the torque generation may be neglected and T_N is the control input. In others, it is not necessary to consider details of electric motor propulsion and it is enough to model the torque generation dynamics by a simple linear equation:

$$\tau\dot{T}_N = -T_N + \gamma T_z, \tag{5}$$

where T_z – the desired torque, is the control variable. Parameters τ, γ may be considered known or unknown, depending on the drive type. It is also assumed that the actual torque T_N may be calculated on-line from the motor current; however, this calculation will vary for different types of motors.

The tracking error will be denoted by

$$e_s = s - s_d. \tag{6}$$

The tracking error dynamics may be derived from (4) and (1)–(3):

$$\dot{e}_s = \frac{R}{Jv}(-RF_a - T_f) - (s+1)\,\frac{1}{Mv}\,(F_a - F_f) + \frac{R}{Jv}T_N - \dot{s}_d. \tag{7}$$

It is assumed that approximate, linearly parameterized models for unknown functions $\mu_a(s)$, $T_f(\omega)$, $F_f(v)$ are available:

$$\begin{aligned} \mu_{mdl}(s) &= \theta_\mu^T \xi_\mu(s), \\ T_{fmdl}(\omega) &= \theta_T^T \xi_T(\omega), \\ F_{fmdl}(v) &= \theta_F^T \xi_F(v), \end{aligned} \tag{8}$$

where the subscript $*_{mdl}$ denotes the output of the model of the function $\mu_a(s)$, $T_f(\omega)$, or $F_f(v)$, respectively, θ_*^T $(* = \mu TF)$ are unknown parameters and ξ_* are known functions of proper dimensions. Approximate models of this type can be obtained from numerical data, by neural or fuzzy modelling [16], or developed by any other method of approximation. Takagi-Sugeno-Kang's fuzzy modelling approach described in [16] can be specifically recommended. This procedure is able to recognize significant inputs and can decide the fuzzy model structure and initial parameters automatically, according to the desired modelling accuracy. For example, the fuzzy model for adhesive coefficient $\mu_{mdl}(s)$ is given by m rules $j = 1, 2, \ldots, m$

$$\text{IF } \ s \ \text{ IS } \ \varphi_j \ \text{ THEN } \ \mu = \mu_j(s) = p_{1j}s + p_{0j}, \tag{9}$$

with membership functions

$$\varphi_j(s) = \frac{1}{1 + \left(\dfrac{s - c_j}{a_j}\right)^{2b_j}}, \tag{10}$$

so that a general description of the model is

$$\mu_{mdl}(s) = \frac{\sum\limits_{j=1}^{m} \mu_j(s)\varphi_j(s)}{\sum\limits_{j=1}^{m} \varphi_j(s)} = \theta_\mu^T \xi_\mu(s), \tag{11}$$

where

$$\begin{aligned} \theta_\mu^T &= [p_{11}, p_{01}, \ldots, p_{1m}, p_{0m}], \\ \xi_\mu(s) &= \frac{1}{\sum\limits_{j=1}^{m} \varphi_j(s)} \begin{bmatrix} s\varphi_1(s) \\ \varphi_1(s) \\ \vdots \\ s\varphi_m(s) \\ \varphi_m(s) \end{bmatrix}. \end{aligned} \tag{12}$$

The fuzzy model may be trained by any suitable method, for example, ANFIS [17]. An exemplary modelling of the adhesive coefficient curve by the fuzzy model is presented in Figs. 2 and 3, where the flexibility offered by fuzzy models is demonstrated.

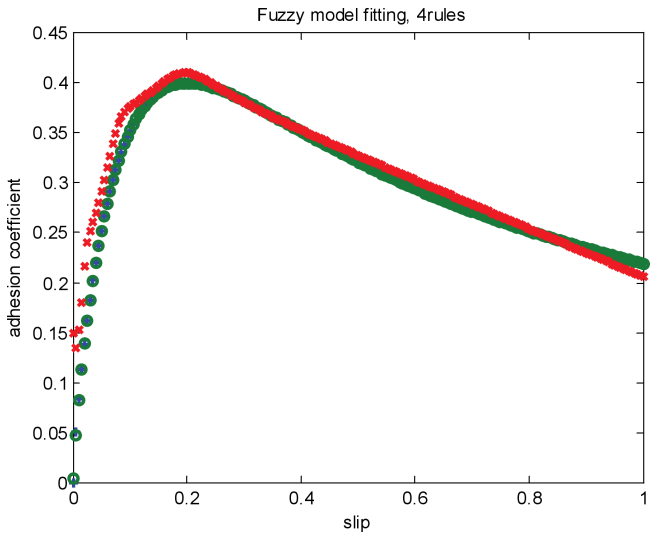

Fig. 2. Adhesion force coefficient fuzzy modelling: input data: +, trained fuzzy model: o, initial fuzzy model: x

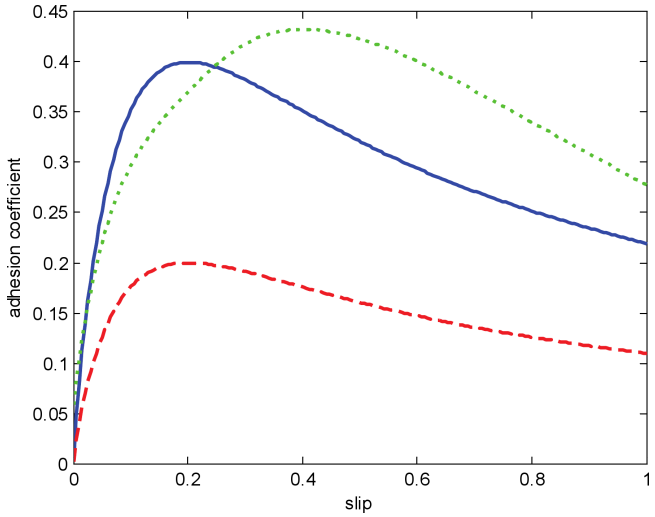

Fig. 3. Adhesion force coefficient fuzzy modelling: three curves obtained by three different sets of consequent parameters $\theta_\mu^T = [p_{11}, p_{01}, \ldots, p_{14}, p_{04}]$ and the same membership functions and rules as in Fig. 2

2.2. Slip tracking control. It is obvious that slip is not defined if linear velocity approaches zero; thus, the application of the derived controller is limited to a bounded interval $0 < v_{\min} < |v| < v_{\max}$.

Let us consider the function

$$f = \frac{1}{v}\left(-\frac{R^2}{J} - (s+1)\frac{1}{M}\right)\mu_a N - \frac{R}{Jv}T_f + (s+1)\frac{1}{Mv}F_f$$

extracted from (7) and let us propose the model of f:

$$\begin{aligned} f_{mdl} &= \theta_f^T \xi_f, \qquad \theta_f^T = \begin{bmatrix} c_\mu & c_{f1} & c_{f2} \end{bmatrix}, \\ \xi_f &= \begin{bmatrix} -\dfrac{1}{v}\left(\dfrac{R^2}{J} + (s+1)\dfrac{1}{M}\right) N_0 \theta_{\mu 0}^T \xi_\mu(s) \\ -\dfrac{R}{Jv}\theta_{T0}^T \xi_T(\omega) \\ (s+1)\dfrac{1}{Mv}\theta_{F0}^T \xi_F(v) \end{bmatrix}, \end{aligned} \tag{13}$$

where R, J, M are defined as in Eqs. (1), (2), N_0 is the nominal normal force, θ^T_{*0} are the nominal values of the parameters in models (8) of $\mu_a(s)$, $T_f(\omega)$, or $F_f(v)$, respectively. The adaptive parameters θ^T_f represent the correcting (proportionality) factors between the actual and nominal values of the components in f. If the initial guess of N_0, $\theta_{\mu 0}$, θ_{T0} and θ_{F0} is precise, the values of c_μ, c_{f1}, c_{f2} will be 1 (and it is the initial condition for adaptation). If the model containing N_0, $\theta_{\mu 0}$, θ_{T0} and θ_{F0} is inaccurate, it will be improved by the adaptation of c_μ, c_{f1}, c_{f2} decreasing the slip tracking error.

The model (13) may be parameterized in various ways; as a matter of fact, the selected parameterization has little impact on control derivation, as long as f_{mdl} is linear in parameters. It follows from our experience that it is sufficient to select one adaptive parameter for each unknown function F_a, T_f, F_f, but one may also apply more adaptive parameters. It is important to assume that there exist constant parameters θ^{*T}_f such that the modelling error is bounded, that is:

$$f = \theta^{*T}_f \xi_f + \varepsilon_f, \qquad |\varepsilon_f| < \varepsilon < \infty, \tag{14}$$

in a compact set of the input variables under consideration. It is not necessary to know ε (neither ε_f), but it is enough to assume that it exists.

Thus, the tracking error dynamics (7) may be represented as

$$\dot{e}_s = \theta^{*T}_f \xi_f - \dot{s}_d + T_N \frac{R}{Jv} + \varepsilon_f. \tag{15}$$

Considering the desired thrust torque

$$T_{Nd} = \frac{Jv}{R}\left(-\theta^T_f \xi_f + \dot{s}_d - K e_s\right), \tag{16}$$

where K is a positive design parameter and denoting

$$e_T = T_N - T_{Nd}, \qquad e_\theta = \theta^*_f - \theta_f, \tag{17}$$

Eqs. (15) and (5) imply that

$$\dot{e}_s = e^T_\theta \xi_f - K e_s + \varepsilon_f + \frac{R}{Jv} e_T, \tag{18}$$

$$\dot{e}_T = -\dot{T}_{Nd} - \frac{1}{\tau}\left(T_{Nd} + e_T\right) + \frac{\gamma}{\tau} T_z. \tag{19}$$

If γ, τ are known, it is possible to apply the control

$$T_z = \frac{\tau}{\gamma}\left(\dot{T}_{Nd} + \frac{1}{\tau}\left(T_{Nd} + e_T\right) - K_T e_T + \alpha\right), \tag{20}$$

where K_T is a positive design parameter. Plugging (20) into (19) results in

$$\dot{e}_T = -K_T e_T + \alpha. \tag{21}$$

Theorem 1. Under the control (20) with

$$\alpha = -e_s \frac{R}{Jv} \tag{22}$$

and adaptive laws

$$\dot{\theta}_f = e_s \Gamma \xi_f - \sigma \|e\| \Gamma \theta_f, \qquad e = \begin{bmatrix} e_s & e_T \end{bmatrix}^T \tag{23}$$

with positive definite Γ and positive σ, trajectories e_s, e_T, e_θ are uniformly ultimately bounded (UUB) and $K_{\min} = \min\{K, K_T\}$ defines the bound for e_s, e_T.

Proof. Consider the Lyapunov function

$$V = \frac{1}{2}\left(e^2_s + e^2_T + e^T_\theta \Gamma^{-1} e_\theta\right). \tag{24}$$

Using (15)–(20), the derivative of V along the system trajectories is derived:

$$\dot{V} = -K e^2_s - K_T e^2_T + e_S \varepsilon_f + \sigma \|e\| e^T_\theta \left(\theta^*_f - e_\theta\right). \tag{25}$$

As $e^T_\theta\left(\theta^*_f - e_\theta\right) = e^T_\theta \theta^*_f - \|e_\theta\|^2 \le \|e_\theta\| \left\|\theta^*_f\right\| - \|e_\theta\|^2 = \|e_\theta\|\left(\left\|\theta^*_f\right\| - \|e_\theta\|\right)$ and $\left\|\theta^*_f\right\| \le \delta$, $e_S \varepsilon_f < \varepsilon \|e\|$, and also $-K e^2_s - K_T e^2_T \le -K_{\min} \|e\|^2$ we get

$$\dot{V} \le -K_{\min} \|e\|^2 + \sigma \|e\| \|e_\theta\| \left(\delta - \|e_\theta\|\right) + \|e\| \varepsilon. \tag{26}$$

Hence, the system derivative is negative if only $\|e\| > \frac{\varepsilon}{K_{\min}}$ and $\|e_\theta\| > \delta$. Negative derivative of the Lyapunov function outside a compact set is sufficient to conclude that the system is stable in UUB sense [19], and that the trajectories will ultimately remain inside the set defined by inequalities $\|e\| < \frac{\varepsilon}{K_{\min}}$, $\|e_\theta\| < \delta$. Therefore it is possible to (arbitrary) decrease $\|e\|$ increasing $K_{\min}$ while keeping the adaptive parameters θ_f bounded. Parameters θ_f are not supposed to identify the unknown θ^*_f, but to cooperate making the whole model (13) accurate enough.

If the exact values of the constant parameters γ, τ are not known precisely, the second adaptive loop must be applied. In this case, we denote the nominal values of the parameters τ_0, $gamma_0$ and introduce

$$p_1 = \frac{1}{\tau_0}, \quad p_2 = \frac{\gamma_0}{\tau_0}, \quad \frac{1}{\tau} = c_1 p_1, \quad \frac{\gamma}{\tau} = c_2 p_2, \tag{27}$$

where c_1, c_2 are constant correcting factors between assumed and real values.

If $a^T = \begin{bmatrix} a_1 & a_2 \end{bmatrix}$ are adaptive parameters and $e^T_a = \begin{bmatrix} \frac{1}{c_2} & \frac{c_1}{c_2} \end{bmatrix} - a^T$ we have

$$\frac{1}{c_2}\frac{d}{dt} e_T = a^T \xi_T + p_2 T_z + e^T_a \xi_T, \tag{28}$$

$$\xi_T = \begin{bmatrix} -\dot{T}_{Nd} \\ -p_1\left(T_{Nd} + e_T\right) \end{bmatrix}. \tag{29}$$

With the control input

$$T_z = \frac{1}{p_2}\left(-a^T \xi_T - K_T e_T + \alpha\right) \quad \alpha = -e_S \frac{R}{Jv} \tag{30}$$

(28) takes the following form:

$$\frac{1}{c_2}\frac{d}{dt} e_T = -K_T e_T + \alpha + e^T_a \xi_T. \tag{31}$$

Theorem 2. Under the control (30) with the adaptive laws (23) and

$$\dot{a} = e_T \Upsilon \xi_T - \sigma \|e\| \Upsilon a, \tag{32}$$

with positive definite Γ, Υ and positive σ, trajectories e_s, e_T, e_θ, e_a are uniformly ultimately bounded (UUB) and $K_{\min} = \min\{K, K_T\}$ defines the bound for e_s, e_T.

Proof. It is analogous to the proof of Theorem 1, but in this instance, we consider the Lyapunov function as being

$$V = \frac{1}{2}\left(e_s^2 + \frac{1}{c_2}e_T^2 + e_\theta^T\Gamma^{-1}e_\theta + e_a^T\Upsilon^{-1}e_a\right). \tag{33}$$

The control proposed in (20) requires the derivative of the desired torque T_{Nd}. This torque was calculated in the first adaptive loop. The same information is required in (30). If the derivative is calculated on-line by a proper discrete filter, the adaptive parameter a_1 also compensates for errors in calculation of the derivative, but the rigorous proof of stability requires strict information on $\dot{T}_{Nd}$. A slightly modified derivation that includes a filter for taking the derivative into account and that allows for proving stability may be presented. This idea is based on the command control filtering approach from the adaptive backstepping control theory [18].

Let us consider a first order filter

$$\dot{z} = -\beta\left(z - T_{Nd}\right) \tag{34}$$

with a design parameter β. When the transient response of the filter vanishes, $z \approx T_{Nd}$, and so $-\beta(z - T_{Nd}) \approx \dot{T}_{Nd}$. It is also evident that $z - T_{Nd}$ is bounded if $\left|\dot{T}_{Nd}\right|$ is bounded. If the initial condition for the filter state variable is $z(0) = T_{Nd}(0)$, then $|z - T_{Nd}| \le \max\left|\dot{T}_{Nd}\right| \beta^{-1}$.

The dynamics of $e_{FT} = T_N - z$ may be described as

$$\frac{1}{c_2}\dot{e}_{FT} = \begin{bmatrix} a_1 & a_2 \end{bmatrix}\xi_{FT} + p_2 T_z + e_a^T\xi_{FT}, \tag{35}$$

$$\xi_{FT} = \begin{bmatrix} \beta\left(z - T_{Nd}\right) \\ -p_1\left(z + e_{FT}\right) \end{bmatrix} \tag{36}$$

and after selection of the control input

$$T_z = \frac{1}{p_2}\left(-a^T\xi_{FT} - K_{FT}e_{FT} + \alpha\right), \quad \alpha = -e_S\frac{R}{Jv} \tag{37}$$

(35) is reduced to

$$\frac{1}{c_2}\frac{d}{dt}e_{FT} = -K_{FT}e_{FT} + \alpha + e_a^T\xi_{FT}. \tag{38}$$

Theorem 3. Under the control (37) and adaptive laws

$$\begin{aligned} \dot{\theta}_f &= e_s\Gamma\xi_f - \sigma\left\|e\right\|\Gamma\theta_f, \\ \dot{a} &= e_{FT}\Upsilon\xi_{FT} - \sigma\left\|e\right\|\Upsilon a, \end{aligned} \tag{39}$$

where

$$e = \begin{bmatrix} e_s & e_{FT} \end{bmatrix}^T, \tag{40}$$

with positive definite Γ, Υ and positive σ, trajectories e_s, e_T, e_θ, e_a are uniformly ultimately bounded (UUB) and $K_{\min} = \min\{K, K_T\}$ defines the bound for e_s, e_{FT}, while K_T and β influence the bound for e_T.

Proof. We consider the Lyapunov function to be:

$$V = \frac{1}{2}\left(e_s^2 + \frac{1}{c_2}e_{FT}^2 + e_\theta^T\Gamma^{-1}e_\theta + e_a^T\Upsilon^{-1}e_a\right). \tag{41}$$

Using (18) and (38)–(40), we calculate the derivative of V along the system trajectories:

$$\begin{aligned} \dot{V} = &-Ke_s^2 - K_{FT}e_{FT}^2 + \sigma\left\|e\right\|e_\theta^T\left(\theta_f^* - e_\theta\right) \\ &+\sigma\left\|e\right\|e_a^T\left(a^* - e_a\right) + e_s\frac{R}{Jv}\left(z - T_{Nd}\right) + e_s\varepsilon_f. \end{aligned} \tag{42}$$

We may formulate a set of inequalities:

$$\begin{aligned} e_\theta^T\left(\theta_f^* - e_\theta\right) &\le \left\|e_\theta\right\|\left\|\theta_f^*\right\| - \left\|e_\theta\right\|^2 = \left\|e_\theta\right\|\left(\left\|\theta_f^*\right\| - \left\|e_\theta\right\|\right), \\ e_a^T\left(a^* - e_a\right) &\le \left\|e_a\right\|\left\|a^*\right\| - \left\|e_a\right\|^2 = \left\|e_a\right\|\left(\left\|a^*\right\| - \left\|e_a\right\|\right), \\ \left\|\theta_f^*\right\| &\le \delta_\theta, \qquad \left\|a^*\right\| \le \delta_a, \\ e_S\left(\varepsilon_f + \frac{R}{Jv}\left(z - T_{Nd}\right)\right) &< \varepsilon\left\|e\right\|, \\ -Ke_s^2 - K_Te_{FT}^2 &\le -K_{\min}\left\|e\right\|^2, \\ K_{\min} &= \min\{K, K_{FT}\} \end{aligned} \tag{43}$$

and hence

$$\begin{aligned} \dot{V} \le &-K_{\min}\left\|e\right\|^2 + \sigma\left\|e\right\|\left\|e_\theta\right\|\left(\delta_\theta - \left\|e_\theta\right\|\right) \\ &+\sigma\left\|e\right\|\left\|e_a\right\|\left(\delta_a - \left\|e_a\right\|\right) + \left\|e\right\|\varepsilon. \end{aligned} \tag{44}$$

Therefore, the system derivative (44) is negative if $\|e\| > \dfrac{\varepsilon}{K_{\min}}$ and $\|e_\theta\| > \delta_\theta$, $\|e_a\| > \delta_a$; thus, trajectories e_s, e_{FT}, e_θ, e_a are uniformly ultimately bounded (UUB) [19] and $K_{\min} = \min\{K, K_{FT}\}$ defines the bound for e_s, e_{FT}. As $e_T = e_{FT} + z - T_{Nd}$, it is also UUB.

2.3. Slip velocity tracking control. The proposed control algorithms, based on a slip tracking approach, require dividing by the actual vehicle velocity. As velocity is a real signal, measured on-line during system operation, any values close to zero may make the control inapplicable.

Slip tracking can also be obtained by slip velocity control. This approach may generate a more robust (numerically) control algorithm, but will require the measurement or calculation of the vehicle acceleration.

Slip velocity is defined by

$$v_s := sv = \omega R - v \tag{45}$$

thus, tracking the desired slip s_d is equivalent to tracking the desired slip velocity $v_{sd} = s_d v$. The desired trajectory derivative must be provided for control and is given as

$$\dot{v}_{sd} = \dot{s}_d v + s_d\dot{v}. \tag{46}$$

If the tracking error for slip velocity is denoted as $e_{vs} = v_s - v_{sd}$, its dynamics may be described by

$$\dot{e}_{vs} = \theta_f^{*T}\xi_f - \dot{v}_{sd} + T_N\frac{R}{J} + \varepsilon_f, \tag{47}$$

where

$$\begin{bmatrix} c_\mu & c_{f1} & c_{f2} \end{bmatrix}\begin{bmatrix} \left(-\dfrac{R^2}{J} - \dfrac{1}{M}\right)N_0\theta_{\mu 0}^T\xi_\mu(s)) \\ -\dfrac{R}{J}\theta_{T0}^T\xi_T(\omega) \\ \dfrac{1}{M}\theta_{F0}^T\xi_F(v) \end{bmatrix} =: \theta_f^T\xi_f \tag{48}$$

$\theta_f^{*T} = \begin{bmatrix} c_\mu^* & c_{f1}^* & c_{f2}^* \end{bmatrix}$ are "optimal" values of parameters leading to the bounded modelling error $|\varepsilon_f| < \varepsilon < \infty$. Note that in this parameterization, adaptive parameters θ_f^T will be able to compensate for the gap between nominal models and the actual values of disturbances $\mu_a(s)$, $T_f(\omega)$, $F_f(v)$, and to cope with the imprecisely know constant parameters $-\frac{R^2}{J} - \frac{1}{M}$, $-\frac{R}{J}$, $\frac{1}{M}$.

Instead of (16), the desired torque

$$T_{Nd} = \frac{J}{R}\left(-\theta_f^T \xi_f + \dot{v}_{sd} - K e_{vs}\right) \tag{49}$$

is used. Plugging (49) into (47) gives

$$\dot{e}_{vs} = e_\theta^T \xi_f - K e_{vs} + \frac{R}{J} e_T + \varepsilon_f \tag{50}$$

while the dynamics of $e_T = T_N - T_{Nd}$ is given by (19), as shown previously. If γ, τ are known, we may apply the control

$$\begin{gathered} T_z = \frac{\tau}{\gamma}\left(\frac{d}{dt}T_{Nd} + \frac{1}{\tau}\left(T_{Nd} + e_T\right) - K_T e_T + \alpha\right), \\ \alpha = -e_{vs}\frac{R}{J} \end{gathered} \tag{51}$$

and proceeding analogously as in the case of slip tracking, we are able to prove the following theorem.

Theorem 4. Under the control (51), (49) and adaptive laws

$$\dot{\theta}_f = e_{vs}\Gamma\xi_f - \sigma \left\|e\right\| \Gamma\theta_f, \quad e = \begin{bmatrix} e_{vs} & e_T \end{bmatrix}^T \tag{52}$$

with positive definite Γ and positive σ and ξ_f defined in (48), trajectories e_{vs}, e_T, e_θ are uniformly ultimately bounded (UUB) and $K_{\min} = \min\{K, K_T\}$ defines the bound for e_{vs}, e_T.

If the exact values of the constant parameters γ, τ are unknown, the second adaptive loop has to be applied as it was done in formulae (27)–(29). We select the control input as

$$T_z = \frac{1}{p_2}\left(-a^T \xi_T - K_T e_T + \alpha\right), \quad \alpha = -e_{vs}\frac{R}{J}. \tag{53}$$

A theorem analogous to Theorem 2 can then be proven.

Theorem 5. Under the control (52), (49) with adaptive laws (52) and

$$\dot{a} = e_T \Upsilon \xi_T - \sigma \left\|e\right\| \Upsilon \tag{54}$$

(ξ_T defined in (29)) with positive definite Γ, Υ and positive σ trajectories e_{vs}, e_T e_θ, e_a are uniformly ultimately bounded (UUB) and $K_{\min} = \min\{K, K_T\}$ defines the bound for e_{vs}, e_T.

Similarly, a control command filtering technique may be introduced as it was in formulae (34)–(36) and following selection of the control input

$$T_z = \frac{1}{p_2}\left(-a^T \xi_{FT} - K_{FT} e_{FT} + \alpha\right), \quad \alpha = -e_{vs}\frac{R}{J}. \tag{55}$$

Theorem 6, analogous to Theorem 3, can be proven.

Theorem 6. Under the control (55), (49) and adaptive laws

$$\begin{aligned} \dot{\theta}_f &= e_{vs}\Gamma\xi_f - \sigma \left\|e\right\| \Gamma\theta_f, \\ \dot{a} &= e_{FT}\Upsilon\xi_{FT} - \sigma \left\|e\right\| \Upsilon a, \end{aligned} \tag{56}$$

$$e = \begin{bmatrix} e_{vs} & e_{FT} \end{bmatrix}^T \tag{57}$$

(ξ_{FT} defined in (36)), with positive definite Γ, Υ and positive σ, trajectories e_{vs}, e_{FT}, e_θ, e_a are uniformly ultimately bounded (UUB) and $K_{\min} = \min\{K, K_T\}$ defines the bound for e_{vs}, e_{FT}, while K_T and β influence the bound for e_T.

The described approaches, i.e., slip stabilization and slip velocity tracking are conceptually equivalent. The primary technical difference is that when slip velocity is tracked, the component $\alpha = -e_{vs}\frac{R}{J}$ appears in control and $\alpha = -e_s\frac{R}{Jv}$ is present if we stabilize the slip. Depending on application details, the velocity range and the measurement technique, the slip velocity control approach may be more robust against measurement noise and outliers.

3. Control performance evaluation

The performance and robustness of the proposed control systems were evaluated by numerous simulation experiments. Some of the results are presented in this paper. The data for the vehicle were taken from a popular locomotive EP07 produced by ZNTK in Poland. One of the bogies was modelled using the following data:

$$M = 20\,000 \text{ kg}, \quad J = 60 \text{ kgm}^2, \quad R = 0.625 \text{ m}. \tag{58}$$

For control purposes, the adhesion coefficient curve was modelled by

$$\mu_a(s) = 2\mu_{\max}\frac{\left(s_{\max}s\right)^{\kappa/2}}{s_{\max}^\kappa + s^\kappa}, \tag{59}$$

which allowed for receiving the curves presented in Fig. 2. The following values were chosen for the nominal parameters: $\kappa = 2$, $\mu_{\max} = 0.4$, $s_{\max} = 0.12$. Rotational friction was modelled as proportional to rotational speed and linear motion resistance as a linear combination of v and v^2.

The disturbances in the bogie model were modelled by look-up tables. Differences between the actual and modelled values of $\mu_a(s)$, $T_f(\omega)$, $F_f(v)$ were roughly 20%. For example, $s_{\max}$ in the plant was 20% smaller than in the model. The normal force of the bogie was disturbed by 10% oscillations, not modelled in the controller. The torque generation was modelled as a first order inertia with a 0.3 s time constant and unity gain, and both were unknown to the controller.

Simulations of many different scenarios were performed, including the braking and accelerating modes of operation. Some of the results are presented in Figs. 4 to 7. The slip tracking algorithm was set to stabilize the desired slip value $s_d = 0.1$, providing a large contact force and effective acceleration for 5 s.

It can be seen from Fig. 7 that adaptation to normal force oscillation was the most important task of the controller. As the adaptive loop is designed to imitate the linear combination with three adaptive parameters, one of them takes the leading role. Likely, the rapid adaptation of only one parameter will be sufficient in this case.

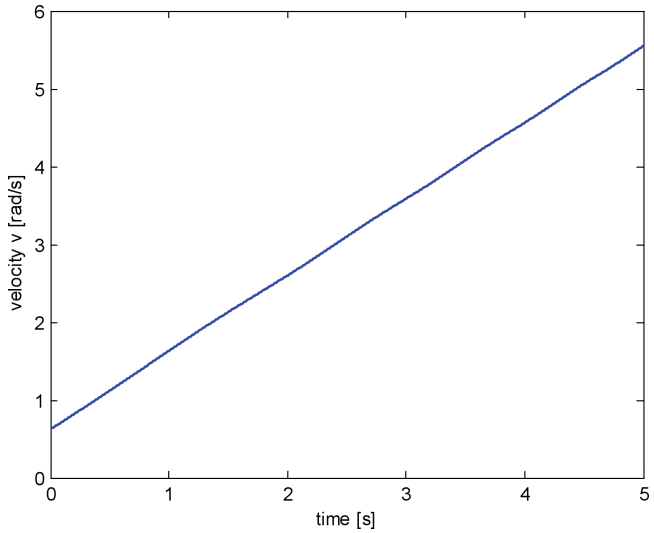

Fig. 4. Acceleration with stabilized slip – slip tracking control (Theorem 3)

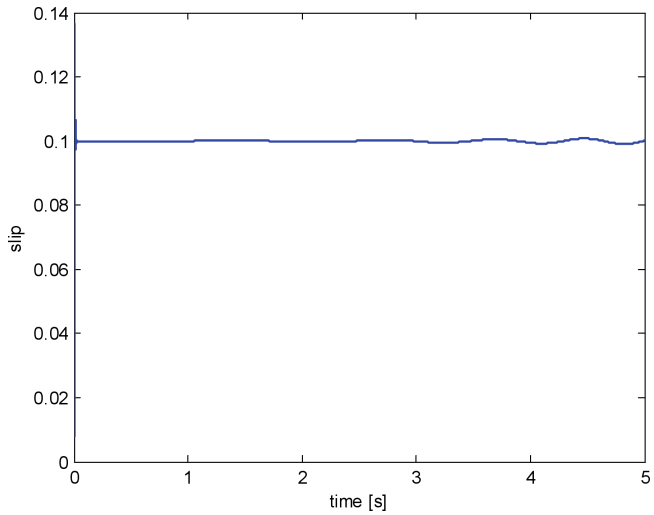

Fig. 5. Slip stabilization on $s_d = 0.1$ – slip tracking control (Theorem 3)

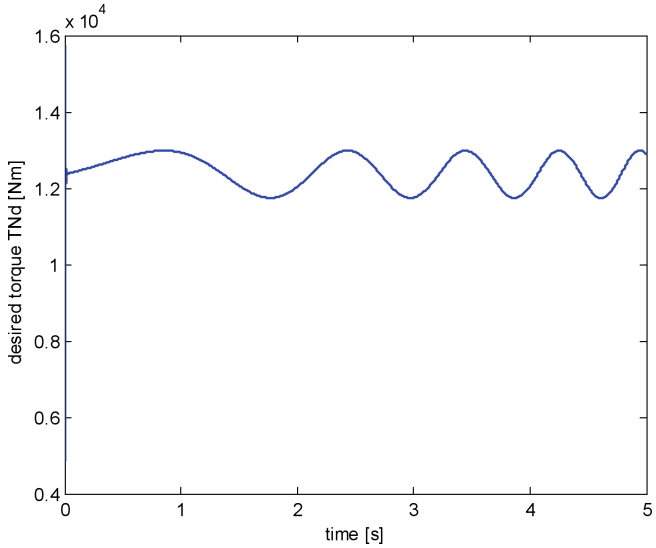

Fig. 6. The desired torque – slip tracking control (Theorem 3)

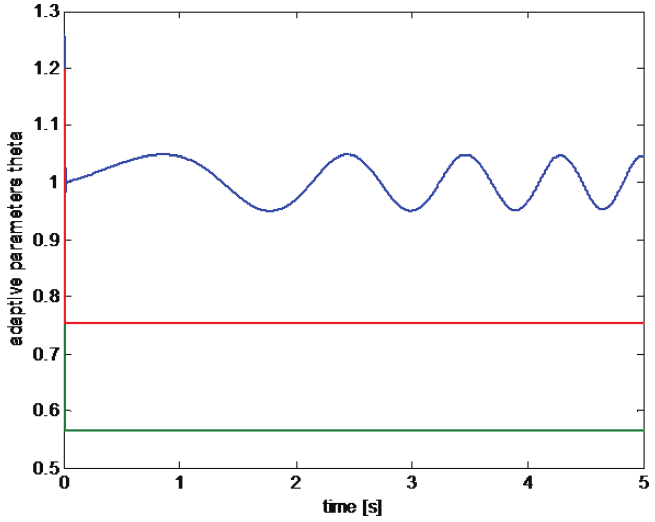

Fig. 7. Adaptive parameters during slip stabilization – slip tracking control (Theorem 3)

The results obtained by the slip velocity tracking algorithm were quite similar, even if moderate (10%) noise was added to the measured velocity.

As practical testing of train control algorithms is technically difficult and expensive, a simple laboratory stand was constructed with a friction gear driven by PMS motors, as shown in Figs. 8 and 9. Normal forces between the wheels are much smaller than those observed between a train wheel and a rail; therefore, the real life adhesive force characteristic is different, but the experiment preserves the typical features of $\mu_a(s)$ curves known for railway transport, with the maximal value of adhesive coefficient obtained for the slip as $s \approx 0.2$. The control algorithms described above were implemented by a signal processor board dSpace 1103 with a sampling time of 50 μs. Algorithms with slip stabilization and slip velocity tracking presented similar behaviour. An exemplary time-history of slip stabilization is presented in Fig. 10. In Fig. 11, the driving wheel rotational speed is plotted together with the receiving wheel speed, multiplied by the gear ratio, while the thrust torque is plotted in Fig. 12.

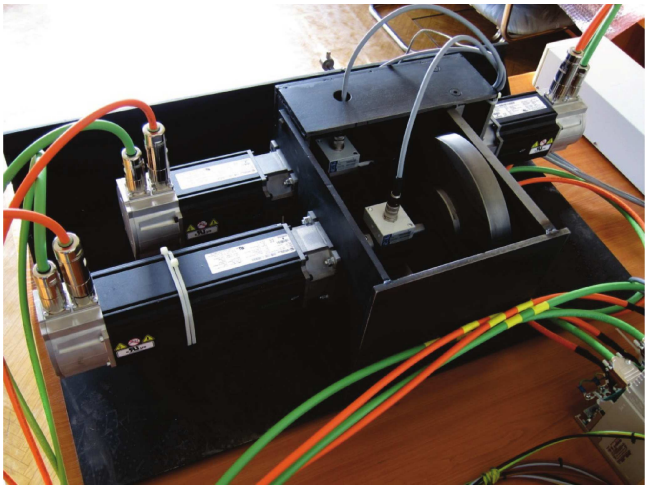

Fig. 8. Laboratory stand with a friction gear driven by PMS motors

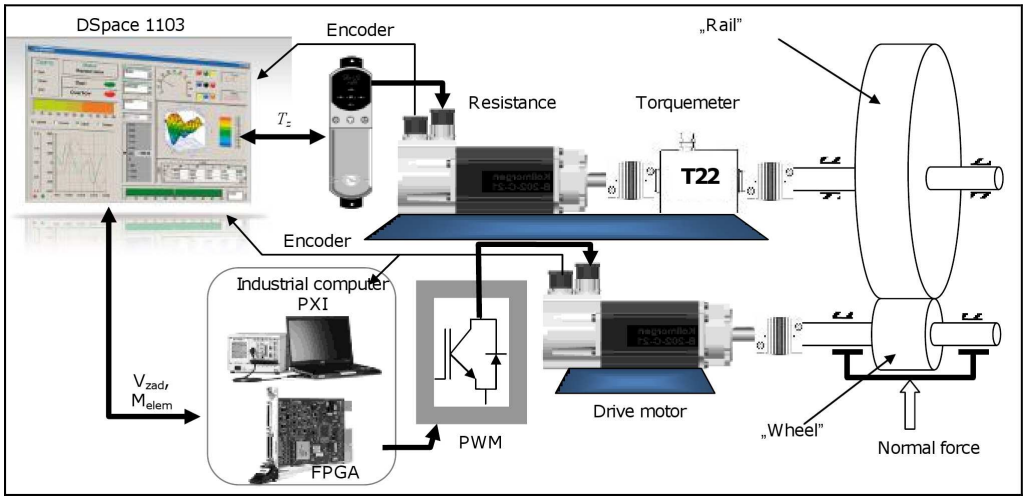

Fig. 9. Diagram of laboratory stand with a friction gear driven by PMS motors

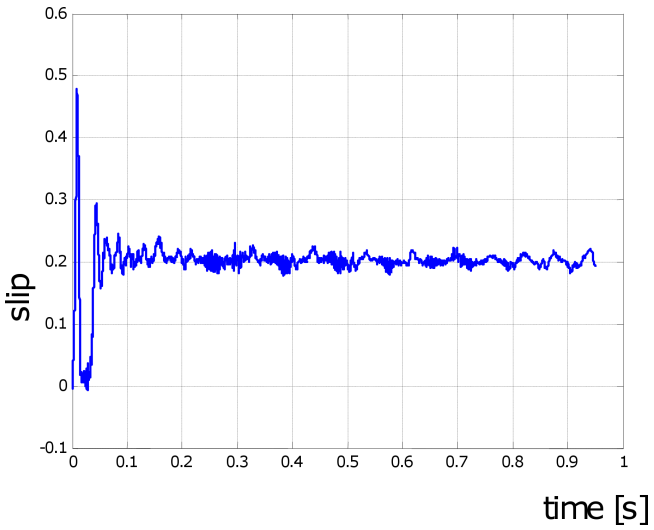

Fig. 10. Slip stabilization in a friction gear driven by PMS motors

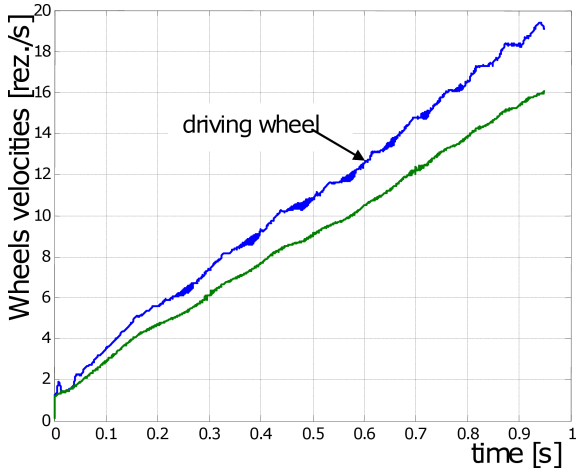

Fig. 11. Wheels rotational speed during acceleration with a stabilized slip

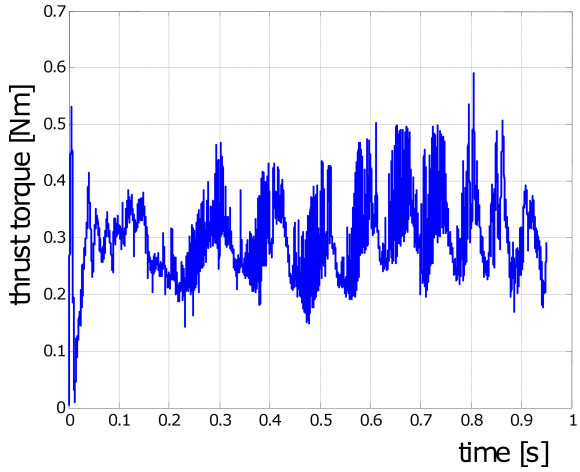

Fig. 12. Thrust torque during slip stabilization

The slip is stabilized sufficiently even in the presence of all the unavoidable measurement noises and errors caused by the digital implementation of the control algorithm.

4. Conclusions

New nonlinear, adaptive controllers were developed that can be successfully applied in railway vehicles to solve the problem of slip or slip velocity tracking or stabilization. The results in the current paper show that it is possible to stabilize the system at the operating point, even if the desired slip value is placed on the negative slope of the slip-adhesion curve. The presented approach allows for considering any disturbances present in the motion dynamics, such as friction and air resistance, and total disturbance compensation is possible. Neither the special structure of the actual slip-adhesion coefficient curve was assumed, nor the special parameterization of the formula describing this curve was required. It is admissible that the implemented models are inaccurate and it is sufficient that the modelling error is bounded.

Additionally, some constant plant parameters may be completely unknown. Naturally, less accurate models require more

effort from the adaptive control loop. The same approach may be used in braking and accelerating the vehicle. The slip tracking control uses typical signals available in modern trains and trams, while a simpler slip velocity tracking algorithm requires a train acceleration signal.

The derived controllers were tested in numerous simulations using various train data. The proposed algorithms were also implemented at the laboratory stand with a frictional gear driven by PMSM. All the experiments – the simulations and the practical implementation – proved that the proposed approach is applicable, possesses attractive features and may present an interesting alternative for existing techniques.

Acknowledgements. This work was supported by the National Science Centre in Poland, the project N N510 646040. The author is grateful to Dr Tomasz Sobieraj for his help regarding the laboratory stand configuration and measurements. The author is grateful to the anonymous reviewers for their numerous suggestions, helping to improve the paper.

REFERENCES

[1] O. Polach, "Creep forces in simulations of traction vehicles running on adhesion limit", *Wear* 258, 992–1000 (2005).

[2] S. Iwnicki, *Handbook of Railway Vehicle Dynamics*, CRC Press, London, 2006.

[3] D-Y. Park, M-S. Kim, D-H. Hwa Ng, Y-J. Kim, and J-H. Lee, "Hybrid re-adhesion control method for traction system of high-speed railway", *IEEE, Proc. Fifth Int. Conf. Electrical Machines and Systems* 2, 739–742 (2001).

[4] M. Spyriagin, K.S. Lee, and H.H. Yoo, "Control system for maximum use of adhesive forces of a railway in a tractive mode", *Mechanical Systems and Signal Processing* 22, 709–720 (2008).

[5] T. Watanabe and M. Yamashita, "Basic study of anti-slip control without speed sensor for multiple motor drive of electric railway vehicles", *IEEE Proc. Power Conversion Conf.* 3, 1026–1032 (2002).

[6] S. Kadowaki, K. Ohishi, T. Hata, N. Iida, M. Takagi, T. Sano, and S. Yasukawa, "Antislip readhesion control based on speed-sensorless vector control and disturbance observer for electric commuter train – series 205-5000 of the East Japan Railway Company", *IEEE Trans. Ind. Electronics* 54, 2001–2007 (2007).

[7] K. Ohishi, Y. Ogawa, I. Miyashita, and S. Yasukawa, "Anti-slip re-adhesion control of electric motor coach based on force control using disturbance observer", *IEEE Industry Applications Conf.* 2, 1001–1007 (2000).

[8] K. Ohishi, S. Kadowaki, Y. Smizu, T. Sano, S Yasukawa, and T. Koseki, "Anti-slip readhesion control of electric commuter train based on disturbance observer considering bogie dynamics", *IEEE Industrial Electronics, IECON 2006 – 32nd Annual Conf.* 1, 5270–5275 (2006).

[9] Rizzo and R.D. Iannuzzi, "Electrical drives for railway traction: observer for friction force estimation", *Power System Technology, Proc. PowerCon 2002, Int. Conf.* 2, 723–726 (2002).

[10] Q. Song, Y.D. Song, and W. Cai, "Adaptive backstepping control of train systems with traction/braking dynamics and uncertain resistive forces", *Vehicle System Dynamics* 49, 1441–1454 (2011).

[11] Q. Song and Y.D. Song, "Neuroadaptive fault-tolerant control of high speed trains with input nonlinearities and actuator failures", *American Control Conf.* 2011, 576–581 (2011).

[12] W. Cai, W. Liao, D. Li, and Y. Song, "Observer based traction/braking control design for high speed trains considering adhesion nonlinearity", *Abstract and Applied Analysis* ID 968017, 17–27 (2014), DOI:10.1155/2014/968017.

[13] J.S. Kim, S.H. Park, J.J. Choi, and H. Yamazaki, "Adaptive sliding mode control of adhesion force in railway rolling stocks", *Sliding Mode Control INTECH*, CD-ROM (2011).

[14] D. Caporale, P. Colaneri, and A. Astolfi "Adaptive nonlinear control of braking in railway vehicles", *Proc. 52 IEEE Conf. Decision and Control* 1, 6892–6897 (2013).

[15] J.J. Kalker, "The computation of three-dimensional rolling contact with dry friction", *Int. J. Numerical Methods in Engineering* 14, 1293–1307 (1979).

[16] J. Kabzinski, "Fuzzy friction modeling for adaptive control of mechatronic systems", in *Artificial Intelligence Applications and Innovations, IFIP Advances in Information and Communication Technology* vol. 381, pp. 185–195, Springer, Berlin, 2012.

[17] J.-S.R. Jang, "ANFIS: adaptive-network-based fuzzy inference system", *Systems, Man and Cybernetics, IEEE Trans.* 23, 665–685 (1993).

[18] W. Dong, J.A. Farrell, M.M. Polycarpou, V. Djapic, and M. Sharma, "Command filtered adaptive backstepping", *Control Systems Technology, IEEE Trans.* 20, 566–580 (2012).

[19] H. Khalil, *Nonlinear Systems*, Macmilan Publishing Co., New York, 1992.